Anion Binding Properties of Reduced and Oxidized Iron-Containing Superoxide Dismutase Reveal No Requirement for Tyrosine 34†

Anne-Frances Miller,*,‡,§ David L. Sorkin,‡ and K. Padmakumar§

Department of Chemistry, The Johns Hopkins University, Baltimore, Maryland 21218, and Department of Chemistry, University of Kentucky, Lexington, Kentucky 40506-0055

Received November 8, 2004; Revised Manuscript Received December 31, 2004

ABSTRACT: We report the first spectroscopic observation of substrate analogue binding to the reduced state of iron superoxide dismutase from *Escherichia coli* (Fe^{2+}SOD) and demonstrate that the pH dependence reflects inhibition of anion binding by ionized Tyr34, not loss of a positive contribution on the part of Tyr34's labile proton. This can also explain the pH dependence of the K_M of Fe^{2+}SOD. Thus, it appears that substrate binding to Fe^{2+}SOD occurs in the second sphere and is not strongly coupled to hydrogen bond donation. Parallel investigations of substrate analogue binding to the oxidized state (Fe^{3+}SOD) confirm formation of a six-coordinate complex and resolve the apparent conflict with earlier nuclear magnetic relaxation dispersion (NMRD) results. Thus, we propose that two F^- ions can bind to the oxidized Fe^{3+}SOD active site, either displacing the coordinated solvent or lowering its exchange rate with bulk solvent. We show that neutral Tyr34's unfavorable effect on binding of the substrate analogue N_3^- can be ascribed to steric interference, as it does not apply to the smaller substrate analogues F^- and OH^-. Finally, we report the first demonstration that HS^- can act as a substrate analogue with regard both to redox reactivity with FeSOD and to ability to coordinate to the active site Fe^{3+}. Indeed, it forms a novel green complex. Thus, we have begun to evaluate the relative importance of different contributions that Tyr34 may make to substrate binding, and we have identified a novel, redox active substrate analogue that offers new possibilities for elucidating the mechanism of FeSOD.

Iron-containing superoxide dismutase (FeSOD)[1] catalyzes the disproportionation of $O_2^{\bullet-}$ to O_2 and H_2O_2 by the following net mechanism:

$$O_2^{\bullet-} + H^+ + Fe^{3+}SOD^{OH^-} \rightarrow O_2 + Fe^{2+}SOD^{H_2O} \quad (1)$$

$$O_2^{\bullet-} + H^+ + Fe^{2+}SOD^{H_2O} \rightarrow H_2O_2 + Fe^{3+}SOD^{OH^-} \quad (2)$$

in which Fe cycles between its +3 and +2 oxidation states, while a coordinated solvent molecule acquires and releases a proton to cycle between OH^- and H_2O, as indicated by the superscripts (*5*, *6*). The Fe ion is ligated by two His residues and one Asp^- as equatorial ligands, with a third His as an axial ligand *trans* to the coordinated solvent (Figure 1, *7*). The coordinated solvent is supported by an H-bond network comprised of amino acids from both domains of FeSOD and extending across the interface to the other monomer of the FeSOD dimer (*7*). Participating residues, including Tyr34, are highly conserved among FeSODs and MnSODs (*7*−*10*).

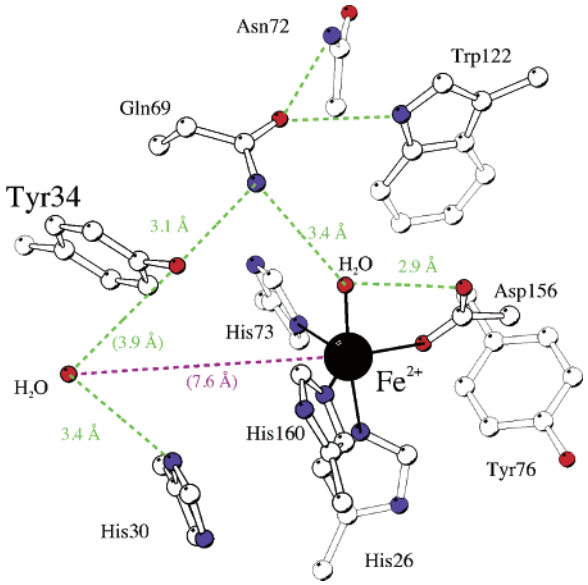

FIGURE 1: Active site of Fe^{2+}SOD, showing proposed H-bonds in green dashed lines, with the distances between participating heavy atoms. A distance larger than 3.5 Å casts in doubt the significance of the indicated H-bond. The distance between Fe^{2+} and the noncoordinated crystallographic water, common to both monomers, is also given in magenta. The coordinates used were 1ISA.pdb of Lah et al. (*7*).

† A.-F.M. is pleased to thank the NIH (GM55210) as well as the NSF (MCB 0129599) for financial support.

* To whom correspondence should be addressed. Phone: 859-257-9349. Fax: 859-323-1069. E-mail: afm@uky.edu.

‡ The Johns Hopkins University.

§ University of Kentucky.

[1] Abbreviations: A_{380} and A_{600}, absorbances at 380 and 600 nm, respectively; CAPS, 3-(cyclohexylamino)-1-propane sulfonic acid; ClO_4^-, perchlorate; Cys, cysteine, DSS, sodium 2,2′-dimethyl-2-silapentane-5-sulfonate; EPR, electron paramagnetic resonance; EXAFS, extended X-ray absorption spectroscopy; FeSOD, iron-containing SOD; H-bond, hydrogen bond; MCD, magnetic circular dichroism; MES, 2-(*N*-morpholino) ethane sulfonic acid; MnSOD, Mn-containing SOD; NMR, nuclear magnetic resonance; NMRD, nuclear magnetic relaxation dispersion; OCN^-, cyanate; PIPES, piperazine-*N*,*N*′-bis(2-ethane sulfonic acid); SCN^-, thiocyanate; SOD, superoxide dismutase; SOR, superoxide reductase, UV/vis, ultraviolet and visible.

10.1021/bi0476331 CCC: $30.25
Published on Web 03/30/2005

Anion binding to (oxidized) Fe^{3+}SOD has been studied for over 20 years. N_3^-, F^-, and a second OH^- have each been shown to coordinate to SOD's Fe^{3+} (*11*−*13*). Furthermore, each of these anions has been shown to inhibit reaction 1 (*6*, *14*). Although ^{1}H NMRD appeared to indicate that N_3^- displaces coordinated solvent to produce a five-coordinate complex while F^- increases the coordination number of Fe^{3+} from five to six (*15*), crystallographic, EXAFS, and MCD studies have shown that N_3^- binding increases the coordination number of Fe^{3+} from five to six (*7*, *13*, *16*, *17*). Superoxide has therefore also been proposed to bind to Fe^{3+}SOD as a sixth ligand in the site that N_3^- occupies, consistent with N_3^-'s behavior as a competitive inhibitor of reaction 1 (*6*).

Other anions including ClO_4^-, SCN^-, CNO^-, Cl^-, NO_3^-, and SO_4^{2-} inhibit Fe^{3+}SOD without coordinating to Fe^{3+} (*6*, *18*, *19*). Kinetic data suggested that these inhibit both reactions 1 and 2, while the Fe^{3+}-coordinating anions inhibit reaction 1 much more than they inhibit reaction 2 (*6*). Nonetheless, even the anions that do not coordinate Fe^{3+} prevent N_3^-, and presumably $O_2^{\bullet-}$, from doing so (*6*). Therefore, it was proposed that noncoordinating anions bind in an additional site, dubbed the "anion binding pocket", and thus prevent productive $O_2^{\bullet-}$ binding (*6*, *12*, *19*). Argese et al. proposed an alternative explanation: that inhibition by noncoordinating anions is simply due to charge screening at the ionic strengths used (*18*).

Maps of changes in NMR chemical shifts of non-active site residues indicate that noncoordinating anions affect the Fe^{2+}SOD protein primarily near the dimer interface (*20*). However, they also show that F^- has additional effects on residues 35−40 that are not produced by other anions (*20*). Our current data extend this finding by demonstrating that the noncoordinating interaction between Fe^{2+}SOD and F^- produces a species with a distinct active site NMR spectrum and a discrete stoichiometry of one F^- per Fe^{2+}SOD monomer, whereas other inhibitory anions do not significantly affect the NMR signals of the active site. Our data provide the first positive spectroscopic evidence for an outersphere anion binding site in the active site and thus the possibility of outersphere binding of substrate to Fe^{2+}SOD.

Both half reactions are inhibited at high pH with p*K*'s near 9 (*6*). The p*K* near 9 affecting the oxidized state of WT-Fe^{3+}SOD reflects coordination of OH^- to Fe^{3+}, but the p*K* of 8.5 affecting the reduced state reflects ionization of Tyr34 (*21*, *25*). Indeed, we find that the oxidized state p*K* persists in Y34F-Fe^{3+}SOD, but the reduced state p*K* is absent (*21*). Although the overall V_{max} of WT-FeSOD does not change, the K_m increases at high pH (*6*, *22*). In the oxidized state, this is attributed to competitive inhibition by OH^- binding (*16*). However, the pH dependence of the reduced state is tentatively ascribed to loss of H-bonding from Tyr 34 or repulsion of substrate by the ion of Tyr34 (*16*, *23*−*25*). Thus, Tyr34 is believed to affect substrate binding for reaction 2.

Substrate should not only bind, but it should also acquire a proton, for reaction 2. This is because electron density flows from Fe^{2+} to $O_2^{\bullet-}$ in reaction 2 instead of from $O_2^{\bullet-}$ to Fe^{3+} in reaction 1. The different directions result, in part, from Fe starting in different oxidation states, but they also require that the substrate be primed for different reactivity in the different half reactions. For the second, protonation of $O_2^{\bullet-}$ is essentially obligatory for this substrate to be amenable to reduction (*26*). Thus, one anticipates that $O_2^{\bullet-}$ should be bound in a nonpolar environment that would elevate its p*K* (but at the cost of binding affinity), or that as part of binding, $O_2^{\bullet-}$ should accept a H bond, which could then develop into outright H^+ transfer in conjunction with electron transfer (*27*).

Tyr34 and His30 are both well positioned to H-bond to substrate binding in the region of the noncoordinated crystallographic solvent in Figure 1 on the left-hand side. Attention in the past has focused on Tyr34, but mutation of that residue to Phe preserved 40% of WT k_{cat}/K_M activity in *Escherichia coli* FeSOD (*21*, *28*). Moreover in human MnSOD, which has a similar active site H-bond network to FeSOD, the k_{cat}/K_M of the Y34F mutant was slightly *higher* than that of the WT, and the K_M of the mutant was effectively 13 times lower than WT-MnSOD's (*8*). Therefore, in an effort to examine the potential significance of Tyr34 and its labile proton to substrate binding, we have devised simpler experiments, comparing binding of several different substrate analogues under conditions in which Tyr34 is neutral or ionized and comparing binding to a mutant in which Tyr34 is replaced by Phe.

Finally, as part of this effort we have discovered a novel substrate analogue: HS^-, which appears to form a coordination complex with Fe^{3+} and engage in redox chemistry with the site. The strong optical signature and redox activity of this species promise exciting new opportunities to probe the reactivity of FeSOD.

MATERIALS AND METHODS

Proteins. WT- and Y34F-FeSOD were expressed and purified as previously described (*24*). The preparations used for this work had specific activities of ≥6000 units/mg for WT- and ≥2400 units/mg for Y34F-FeSOD.

EPR Spectroscopy. Data were collected on an X-band EMX EPR spectrometer. For temperatures of 110 K, an N_2 flow cryostat was used, and data were collected at 9.473 GHz at a nominal power of 8 mW, whereas at 4.2 and 16 K an Oxford ESR900 He flow cryostat was used, and data were collected at 9.512 GHz at a nominal power of 1 mW. 10 G modulation amplitude at 100 kHz was used in all cases, and sweep widths of 0−6000 or 0−10000 G were collected in 11 min scans of 8k points. Approximately 0.5 mM Fe^{3+}SOD in 25 mM phosphate buffer at pH 7.5 was supplemented with stock solutions of NaN_3 or KF adjusted to pH 7.5, to produce final concentrations of 30 mM N_3^- or 33 mM F^-, respectively. For studies with HS^- (33 mM final), no buffer or other salts were used. Samples in 4 mM quartz EPR tubes were frozen by immersion in liquid N_2 and stored between uses at −70 °C.

NMR Spectroscopy. With the exception of the spectra in Figure 4, all data were collected on a Bruker AMX 300 MHz spectrometer at 303 K. Spectra in Figure 4 were collected on a Varian Inova 400 MHz spectrometer at 303 K. FeSOD samples at approximately 1 mM were degassed and then reduced in NMR tubes with a 2-fold stoichiometric excess of sodium dithionite (in 0.1 M KOH). They were then flame sealed, sealed with a septum for quick observations, or sealed with a valve and septum in the case of titrations. pHs were determined by the use of internal indicator molecules' chemical shifts, as previously described (*24*), for data in Figures 2, 3, and 5, or using a microelectrode prior to

reduction and again after collection of NMR spectra, for Figure 4. For the initial identification of anions able to bind to Fe^{2+}SOD, FeSOD was transferred to unbuffered ^2H_2O by repeated dilution and reconcentration in a centricon. Neutral pH was maintained via the buffering capacity of the protein. A total of 50 μL of 500 mM NaN_3, CH_3OH, KF, or KSCN in ^2H_2O were added to 450 μL of 1 mM FeSOD prior to reduction with a 2-fold stoichiometric excess of dithionite in KOH dissolved in ^2H_2O to 0.1 M.

The super-WEFT pulse sequence of Inubishi and Becker (*29*) was used to observe paramagnetically shifted and broadened resonances from active site residues. The pulse sequence was implemented at 300 MHz with a 15 ms relaxation delay, a 35 ms delay between pulses, and a 25 ms acquisition time. At 400 MHz (Figure 4), a delay of 40 ms was used between pulses, but otherwise the same observation methods were used. Water was subjected to continuous wave saturation during both delays. 300 MHz data were processed with some −20 Hz Lorentz line narrowing and 0.1 s Gaussian line broadening prior to Fourier transformation onto 16k points for a 62 500 Hz sweep width. 400 MHz data were subject to up to −50 Hz Lorentz line narrowing and 20 ms Gaussian broadening prior to Fourier transformation onto 16k points for 125 kHz sweep width.

pH and F⁻ Binding Titrations. The [F⁻] and pH dependence study of Fe^{2+}SOD entailed four separate titrations, all in 90% ^1H_2O/10% ^2H_2O. These included one titration with 0.1 M KOH of unbuffered Fe^{2+}SOD containing no F⁻, a titration with 0.1 and 0.5 M KF of Fe^{2+}SOD in 25 mM potassium phosphate buffer initially at pH 7.4, a titration with 0.1 and 1.0 M KF of Fe^{2+}SOD in 25 mM potassium pyrophosphate buffer initially at pH 9.5, and a titration with 0.1 M KOH of unbuffered Fe^{2+}SOD initially containing 199 mM KF. For each data point, two NMR spectra were recorded, a super-WEFT to observe the Fe^{2+}SOD active site, and a spin−echo to observe internal pH indicators (*24*).

The Y34F-Fe^{2+}SOD samples shown in Figure 4 were in 25 mM potassium phosphate, at pH 7.4 or 10.6, and 0 mM or 500 mM KF, as indicated in the figure. KF was added as a 5 M stock solution at pH 7.4, and the pH was adjusted by adding 0.1 M KOH, prior to reduction of the sample. For the titration of F⁻ binding, Y34F-Fe^{2+}SOD initially in 25 mM potassium phosphate buffer was titrated with 0.1, 1.0, and 5.0 M KF until a KF concentration of 279 mM was attained. The sample was then titrated with 0.1 M KOH to pH 9.8. Each responsive active site chemical shifts' dependence on [F⁻] was analyzed according to eq 3

$$\delta_{obs} = \delta_o + (\delta_F - \delta_o)[Fe^{2+}SOD{\cdot}F^-]/[Fe^{2+}SOD]_T \quad (3a)$$

where δ_{obs}, δ_o, and δ_F are the chemical shifts of a resonance observed at some [F⁻], at 0 mM F⁻, and at saturating [F⁻], respectively, and the fraction of Fe^{2+}SOD with F⁻ bound, $[Fe^{2+}SOD{\cdot}F^-]/[Fe^{2+}SOD]_T$, is

$$[Fe^{2+}SOD{\cdot}F^-]/[Fe^{2+}SOD]_T = [F^-]/(K_d + [F^-]) \quad (3b)$$

where $[Fe^{2+}SOD]_T$ is the total Fe^{2+}SOD concentration and $[Fe^{2+}SOD{\cdot}F^-]$ is the concentration with F⁻ bound.

The (oxidized) Fe^{3+}SOD NMR samples were in 90% ^1H_2O/10% ^2H_2O with 10 mM MES pH 6.0 and either 10 mM NaCl (K_d = 71 mM (*6*)), 10 mM KF (K_d = 2 mM (*11*)), or 5 mM NaN_3 (K_d = 1.5 mM). The complex with OH^- bound was produced by adjusting to pH 9.3 a sample of Fe^{3+}SOD in 100 mM NaCl and buffered with 50 mM $NaBO_4$. The super-WEFT sequence described above was used to observe these samples.

UV/Visible Titrations. All UV/vis spectra were recorded at 25 °C using a Hewlett-Packard 8452A diode array spectrophotometer. Titration of Fe^{3+}SOD with 0.1 M KOH was unsuccessful due to precipitation and irreproducibility. Instead, two 800 μL portions of Fe^{3+}SOD which had been dialyzed against deionized water were mixed with buffer, one with 200 μL of 50 mM PIPES, 50 mM CAPS, 50 mM NaCl at pH 6.6 and the other with 200 μL of 50 mM PIPES, 50 mM CAPS, 50 mM NaCl at pH 10.6. A UV/vis spectrum of each sample was recorded. Then, an aliquot of each sample was removed and mixed with the other sample, and the pH and spectrum of each were again recorded. This was repeated until the pHs of the two samples converged. In addition to preventing precipitation due to locally high hydroxide concentrations, this method had the additional benefit of eliminating dilution of protein by the titrant.

Protein solutions for all UV/vis N_3^- and F⁻ titrations contained 25 mM potassium phosphate buffer, pH 7.4. Azide was added as 0.1 M NaN_3 in the case of Y34F-Fe^{3+}SOD, while both 0.1 and 0.5 M NaN_3 were used for the WT-. F⁻ was added as both 0.1 and 1.0 M KF.

In the case of N_3^- binding to Y34F-Fe^{3+}SOD, where binding was tight, eqs 4 and 5 were used to fit the titration data. $A = \Sigma(\epsilon c l)$, where A is the absorbance at some wavelength, ϵ is the extinction coefficient (a constant for the species indicated), c is the concentration of the species, and our path length l is 1 cm.

$$A = \epsilon_1[Fe^{3+}SOD] + \epsilon_2[Fe^{3+}SOD{\cdot}L] \quad (4)$$

$$[Fe^{3+}SOD{\cdot}L] = (K_d + L_T + Fe^{3+}SOD_T - ((K_d + L_T + Fe^{3+}SOD_T)^2 - 4L_T Fe^{3+}SOD_T)^{1/2})/2 \quad (5)$$

where L_T and $Fe^{3+}SOD_T$ represent the total concentrations of ligand (bound and free N_3^-) and Fe^{3+}SOD, $[Fe^{3+}SOD]$ and $[Fe^{3+}SOD{\cdot}L]$ represent the concentrations of free and ligand-bound Fe^{3+}SOD, and $[Fe^{3+}SOD] = Fe^{3+}SOD_T - [Fe^{3+}SOD{\cdot}L]$. Absorbance data points could not be corrected for dilution because this equation is not linear in $Fe^{3+}SOD_T$, so a correction was made by substituting $Fe^{3+}SOD_T = Fe^{3+}SOD_{T,0}(1 - L_T/L_S)$, where L_S is the concentration of the ligand stock solution and $Fe^{3+}SOD_{T,0}$ is the initial concentration of Fe^{3+}SOD. In the cases of the other titrations, where the weak binding approximation holds, the simplification $[L] = L_T$ could be made. Thus eq 6 was used for N_3^- binding to WT-Fe^{3+}SOD

$$[Fe^{3+}SOD{\cdot}L] = Fe^{3+}SOD_T[L]/(K_d + [L]) \quad (6)$$

and eq 7 was used to describe F⁻ binding to two sites

$$A = (\epsilon_1 + \epsilon_2[L]/K_{d1} + \epsilon_3[L]^2/K_{d1}K_{d2})Fe^{3+}SOD_T/(1 + [L]/K_{d1} + [L]^2/K_{d1}K_{d2}) \quad (7)$$

after correcting the absorbance data for dilution.

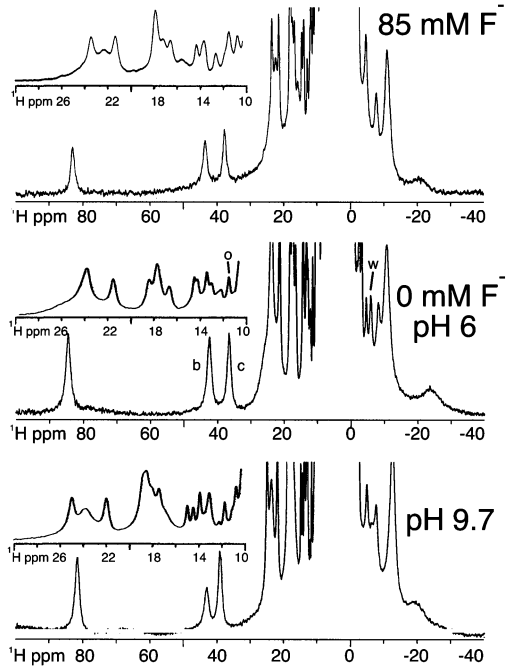

FIGURE 2: Comparison of the effects of high pH and F^- on the active site ^1H NMR spectrum of Fe^{2+}SOD. The super-WEFT spectrum of pH 7 WT Fe^{2+}SOD with 85 mM F^- (top), without F^- bound at pH 6 (middle), and without F^- at high pH (pH = 9.7, bottom) are compared at 30 °C and 300 MHz. F^- was supplied as a KF stock solution to a final concentration of 85 mM vs the K_d of 42 mM (Table 1) and the pH was raised by adding KOH. The active site ^1H NMR spectrum has been shown to be the same at pH 6 and 7 (*24*), so the differences between the top and middle spectra represent the effects of F^-. Resonances used to monitor F^- binding are indicated for the middle pair of spectra by lower case letters according to the notation in ref *33* (see also Figure 3 and Table 1).

For experiments with hydrogen sulfide (H_2S), FeSOD was dialyzed against dionized water to remove all buffers and other salts, and the pH was adjusted to approximately pH 7.4 with 0.1 M KOH. H_2S ($pK_2 = 12.9$ and $pK_1 = 7.0$) was added as a 0.5 or 0.1 M stock solution of Na_2S adjusted to pH 7.4 or pH 8, respectively, with HCl.

RESULTS

Anion Binding to (Reduced) Fe^{2+}SOD. Prior to this work, no distinct anion-bound form of reduced Fe^{2+}SOD's active site had been observed spectroscopically, although substrate must somehow interact with Fe^{2+}SOD.[2] This was in part because Fe^{2+}SOD is UV/vis- and perpendicular mode EPR-silent due to the S = 2 spin state of Fe^{2+}. Fe^{2+} sites are amenable to MCD and Mössbauer spectroscopy. However, MCD studies found no evidence for N_3^- or F^- binding to Fe^{2+}SOD (*30*), possibly because MCD is much more sensitive to metal ion coordination events than second-sphere events such as binding to protein residues. By contrast, ^1H NMR is very sensitive to events affecting Fe^{2+}SOD active site amino acids (*21*, *24*, *31*, *32*), resonances have been assigned to all the ligands and many of the second-sphere residues (*33*), and resonances of residues within ≈8 Å of Fe^{2+} can be monitored semi-selectively by virtue of their paramagnetically enhanced relaxation rates (*29*).

[2] The complex formed by NO and Fe^{2+}SOD is most accurately described as Fe^{3+}SOD·NO^- (*1*) and thus most properly represents oxidized Fe^{3+}SOD, not the reduced state.

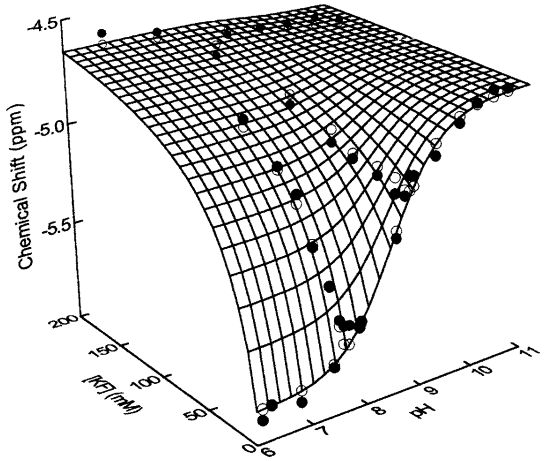

FIGURE 3: Titration of Fe^{2+}SOD with F^- and OH^-. pH and [KF] dependence of the chemical shift of a WT Fe^{2+}SOD His30 β proton resonance, w (marked on the right-hand side of the middle spectrum in Figure 2). Data were fit with eq 8, and parameters of the fit are given in Table 1. Both the experimental values (●) and those predicted by the model (○) are shown. The data were plotted and fit using the Systat package.

We tested the anions N_3^-, F^-, and SCN^-, each at a concentration of 50 mM, but only F^- affected the ^1H NMR super-WEFT spectrum of the reduced Fe^{2+}SOD active site. Similarly, methanol, which was found to coordinate to the Fe^{2+} of lipoxygenase (*34*), had no effect on the Fe^{2+}SOD super-WEFT spectrum at a concentration of 50 mM. Thus, although some anions that inhibit FeSOD do not affect the reduced active site, F^- does, indicating that the effect observed by NMR is somewhat specific, and not simply that of ionic strength.

At pHs below ~8.5, F^- was found to cause changes of up to 3 ppm in the chemical shifts of paramagnetically shifted resonances of Fe^{2+}SOD (Figure 2). No significant changes in resonance line widths were observed in the course of the F^- titration, and the chemical shift changes were similar in magnitude to those observed upon ionization of Tyr34 (*24*). This indicates that interaction with F^- also corresponds to a second-sphere event.

As the pH was increased, F^- had a diminishing influence on active site chemical shifts, until no effect could be detected, above pH 10. Previous work identified Tyr34 as responsible for the pH dependence of the Fe^{2+}SOD active site (*21*, *24*, *35*). Therefore, to elucidate the relationship between F^- binding and Tyr34, a series of F^- and pH titrations were performed, yielding an array of data spanning F^- concentrations from 0 to 199 mM and pH 5.6 to 10.6 (Figure 3). Since high pH supresses F^- binding, the data were fit to the following competitive binding model: mutually exclusive deprotonation of an ionizable group and binding of F^- (Scheme 1).[3]

Scheme 1: Model for F^- Binding in Competition with Deprotonation of Fe^{2+}SOD

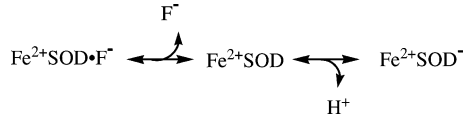

Data were fit with eqs 8a−c, in which the observed chemical shift (δ_{obs}) represents a population-weighted average

Table 1: Parameters Describing the pH and F^- Titration of WT Fe^{2+}SOD, as Monitored by NMR

peak (assignment)[a]	δ_A (ppm)	δ_{HA} (ppm)	δ_F (ppm)	K_d (mM)	pK
b (His 160 Nδ1)	42.40	43.15	44.13	49 ± 6	8.41 ± 0.06[b]
c (His 73 Nδ1)	39.24	36.51	38.32	44 ± 4	8.46 ± 0.02
o (Trp 77 ζ3)	11.76	11.43	11.85	43 ± 5	8.60 ± 0.04
w (His 30 β)	−4.70	−5.84	−4.44	35 ± 5	8.41 ± 0.04
average[c]				42 ± 5	8.47 ± 0.04

[a] Assignments from Sorkin and Miller (*33*); the resonances used are labeled in Figure 2. [b] Standard error of the fit, not including a 0.06 pH unit uncertainty expected based on the performance of the pH electrode used in the calibration of the NMR pH indicators. [c] (Uncertainty^{-2})-weighted average.

of the chemical shifts of F^--bound protonated Fe^{2+}SOD (δ_F), protonated free Fe^{2+}SOD (δ_{HA}), and deprotonated free Fe^{2+}SOD (δ_A), with the three species in fast exchange with one another:

$$\delta_{obs} = \delta_{HA} + (\delta_F - \delta_{HA})[FeSOD{\cdot}F^-]/[FeSOD]_T + (\delta_A - \delta_{HA})[FeSOD^-]/[FeSOD]_T \quad (8a)$$

where the fraction of F^--bound Fe^{2+}SOD is given by

$$[FeSOD{\cdot}F^-]/[FeSOD]_T = [F^-]/(K_d(1 + 10^{pH-pK}) + [F^-]) \quad (8b)$$

and the fraction of deprotonated Fe^{2+}SOD is given by

$$[FeSOD^-]/[FeSOD]_T = 10^{pH}/(10^{pK}(1 + [F^-]/K_d) + 10^{pH}) \quad (8c)$$

The above model provides a good fit to the chemical shifts of all resolved resonances that experience significant F^- and pH dependencies ($R^2 \geq 0.99$, Figure 3) and yields a K_d of 42 mM for F^- binding and a pK of 8.47 for the ionizable group, from the (uncertainty^{-2})-weighted average of the K_d and pK values for each resonance (Table 1). This pK value is in remarkably good agreement with the pK of 8.50 for Tyr 34 (*24*), suggesting that Tyr34 is responsible for the pH dependence of F^- binding. The K_d of F^- binding to Fe^{2+}SOD is large relative to the K_d of 2 mM for Fe^{3+}SOD (*11*) but could nonetheless contribute to inhibition of FeSOD, as it is similar to the K_I near 33 mM (*11*).

Significance of Tyr34 for F^- Binding to Fe^{2+}SOD. To test the hypothesis that loss of F^- binding at high pH reflects a requirement for Tyr34's phenolic H^+, we characterized F^--binding to Fe^{2+}SOD in which Tyr34 was mutated to Phe (Y34F-Fe^{2+}SOD). Near neutral pH, the effect of F^- on the active site NMR spectrum was similar to that observed for WT-Fe^{2+}SOD (Figure 4). Thus, a qualitatively similar event is implied: F^- binding outside the coordination sphere. An NMR-monitored titration yielded a K_d of 66 ± 8 mM, based on the (uncertainty^{-2})-weighted average of the K_d values obtained for several resonances (Table 2, Figure 5). This value is similar to the K_d of 42 mM obtained for WT-Fe^{2+}SOD, arguing against a requirement for Tyr34's phenolic H for anion binding.

[3] Mathematically, this is equivalent to OH^- and F^- binding in competition with one another.

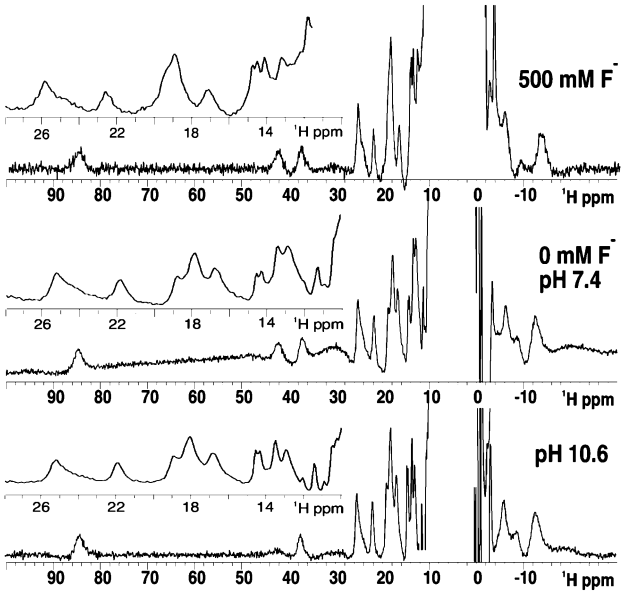

FIGURE 4: Comparison of the effects of high pH and F^- on the active site ^{1}H NMR spectrum of Y34F-Fe^{2+}SOD. The super-WEFT spectrum of pH 7.4 Y34F-Fe^{2+}SOD with 500 mM F^- (top), without F^- at pH 7.4 (middle), and without F^- at high pH (pH $\approx$ 10.6, bottom) are compared at 30 °C and 400 MHz. F^- was supplied as a KF stock solution to a final concentration of 500 mM vs the K_d of 66 mM (Table 2) and the pH was raised by adding KOH. Although the pHs reported here are not the same as those in Figure 2, they show the active site spectrum to be pH independent, with the correlary that any other pHs in the stability range of Y34F-Fe^{2+}SOD would also produce the same spectrum and thus that these spectra can be compared with those in Figure 2.

Table 2: Parameters Describing F^- Binding to Y34F-Fe^{2+}SOD, as Monitored by NMR[a]

peak (assignment)[b]	δ_o (ppm)	δ_F (ppm)	K_d (mM)
c (His 73 Nδ1)	37.18	38.03	108 ± 9
f (?)	21.71	22.34	73 ± 9
o (Trp 77 ζ3)	11.41	11.81	58 ± 5
w (His 30 β)	−5.37	−4.89	43 ± 9
average[c]			66 ± 8

[a] Observed chemical shifts, δ_{obs}, vs [F^-] were fit to eq 8 simplified in accordance with the absence of pH dependence; $\delta_{obs} = \delta_o + (\delta_F - \delta_o)[FeSOD{\cdot}F^-]/[FeSOD]_T$, where δ_o is the chemical shift of free Y34F-Fe^{2+}SOD and the other symbols are as defined above. [b] By comparison with the wild-type spectrum and assignments, where unambiguous. [c] (Uncertainty^{-2})-weighted average.

The chemical shifts of active site F^-·Y34F-Fe^{2+}SOD resonances changed very little when the pH was adjusted to 9.8 in the presence of 200 mM KF (Figure 5). This is consistent with the pH independence of the active site NMR spectrum of Y34F-Fe^{2+}SOD in the absence of F^- (Figure 4), and unlike the behavior of WT-Fe^{2+}SOD (*21*, *24*). Thus, in Y34F-Fe^{2+}SOD, F^- binding is retained at high pH, supporting the proposal that Tyr34 is responsible for the pH dependence of F^- binding in WT-Fe^{2+}SOD.

Anion Binding to (Oxidized) Fe^{3+}SOD. OH^-, F^-, and N_3^- have long been known to coordinate to the Fe^{3+} of oxidized Fe^{3+}SOD (*7*, *11*, *13*). Since they compete with one another and with substrate binding (*6*), they are considered to be substrate analogues with respect to Fe^{3+}SOD. We have now investigated the significance of Tyr34 for substrate binding

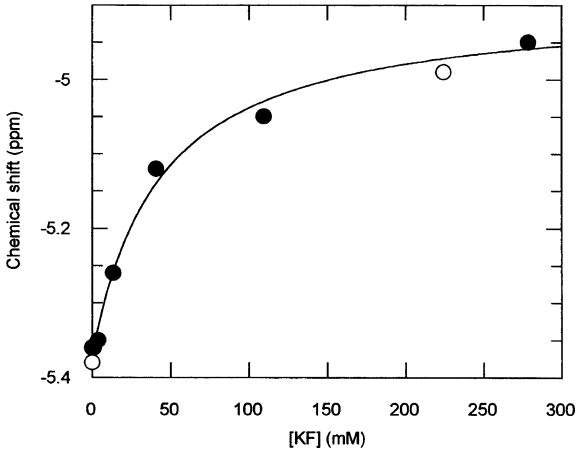

FIGURE 5: F^- binding to Y34F-Fe^{2+}SOD, based on the [KF] dependence of the chemical shift of a Y34F-Fe^{2+}SOD His 30 β proton resonance, w, at pH 7 (●), and at pH 9.8 (○). Data were fit with eq 8 simplified in accordance with the absence of pH dependence; $\delta_{obs} = \delta_o + (\delta_F - \delta_o)[FeSOD{\cdot}F^-]/[FeSOD]_T$, where δ_o is the chemical shift of free Y34F-Fe^{2+}SOD, and parameters of the fit are given in Table 2.

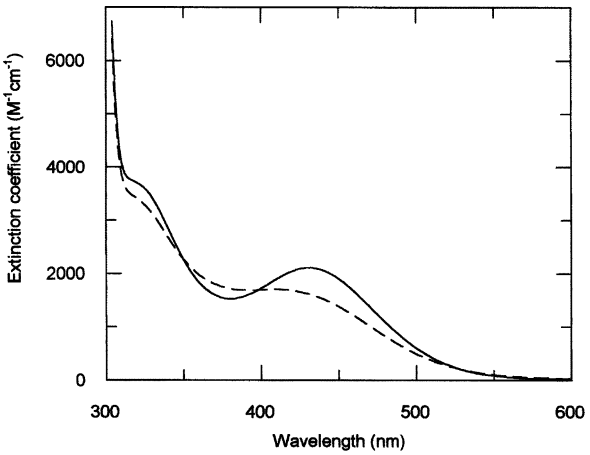

FIGURE 6: N_3^- binding to Fe^{3+}SOD. UV−visible spectra of azide-saturated WT- (dashed line) and Y34F-Fe^{3+}SOD (solid line), at ≈0.3 mM Fe^{3+}SOD in pH 7.4, 25 mM phosphate buffer.

to Fe^{3+}SOD by characterizing anion binding to oxidized Y34F-Fe^{3+}SOD.

Near neutral pH the UV/vis spectra of WT- and Y34F-Fe^{3+}SOD are nearly identical (data not shown), suggesting that the metal site is unaffected by the mutation, in agreement with EPR and NMR data (*21*). However upon N_3^- binding, Y34F-Fe^{3+}SOD displays a more pronounced band near 430 nm than does the WT- (Figure 6). Since this band is assigned to an N_3^-−Fe^{3+} ligand-to-metal-charge-transfer (*17*), its apparent greater strength in Y34F-Fe^{3+}SOD may indicate that N_3^- has a greater tendency to be coordinated to Fe^{3+} in Y34F- than in WT-Fe^{3+}SOD (*17*). Thus, it appears that in the absence of Tyr34's hydroxyl, N_3^- can coordinate to Fe^{3+} better.

On the basis of optically monitored titrations and eqs 4 and 5, we find that a single N_3^- binds to Y34F-Fe^{3+}SOD with a K_d of 80 ± 15 μM, while WT-Fe^{3+}SOD has a single K_d of 1.5 mM, in good agreement with previously obtained values which range from 1.5 to 2.2 mM (Table 3; *6*, *11*). The 19-fold tighter binding we observe for Y34F-Fe^{3+}SOD correlates well with a previous observation that N_3^- inhibits Y34F-FeSOD with a 20-fold lower K_I than its K_I for WT-FeSOD (*28*), and 20-fold tighter N_3^- binding for Y34F-Fe-substituted-MnSOD than WT-Fe-substituted-MnSOD (*9*). Tighter binding to Y34F-Fe^{3+}SOD of the larger-than-substrate analogue N_3^- is likely due to relief of steric repulsion between Tyr34's OH and N_3^-. This hypothesis is supported by crystallographic studies, which find that N_3^- displaces Tyr34 by 0.4 Å (*7*).

Table 3: Summary of the Parameters of Anion Binding to Fe^{3+}SOD

ligand	Fe^{3+}SOD	K_{d1} (mM)	K_{d2} (mM)[c]
F^-	WT	2.0[a]	42
F^-	Y34F	10	>200
N_3^-	WT	1.5	NA
N_3^-	Y34F	0.081	NA
OH^-	WT	NA[b]	8.61[c]
OH^-	Y34F	NA[b]	~8.8[c]

[a] From Slykhouse & Fee (*11*). [b] One solvent molecule is thought to remain coordinated across the pH range. [c] OH^- binding constants are expressed as p*K*'s.

The smaller-than-substrate analogues F^- and OH^- provide a test of the above proposal. We find that F^- binds more loosely to Y34F-Fe^{3+}SOD than to the WT. Initial studies of F^- binding found that two F^- ions bind to WT-Fe^{3+}SOD with K_d's of 2.0 and 42 mM (*11*). Later work finds that if a small amount of organic solvent is added to the protein solution, only one K_d of 6.9 mM is observed (*6*). Our titration data of Y34F-Fe^{3+}SOD did not fit to a single K_d (we did not include any organic solvent in the protein solution). Thus, we obtain two K_d's, one of 10 ± 2 mM, and the other too high to accurately measure at readily obtainable F^- concentrations but greater than 200 mM (Table 3).

The p*K* of OH^- binding to WT-Fe^{3+}SOD was previously measured by EPR and UV/vis monitored titration with OH^- (*12*). The p*K* value obtained by this method was 9.3 ± 0.3 compared to 8.6 ± 0.3 obtained from the pH dependence of the K_d of N_3^- binding (*12*). However, the authors noted an unusual amount of scatter in their data as well as precipitation upon each addition of OH^-. Moreover, when we repeated the titration using OH^- to increase pH, we observed the same precipitation and irreproducibility problems too. However, use of the "aliquot swapping" technique described in the methods section eliminated precipitation and yielded reproducible results (Figure 7). Two independent titrations yielded p*K*'s of 8.56 ± 0.04 and 8.65 ± 0.04 with an average value of 8.61 ± 0.04. This is consistent with an earlier prediction (*6*) that the active site p*K*'s of Fe^{2+}- and Fe^{3+}SOD are no greater the 0.3 units apart, as the active site (Tyr34) p*K* of reduced Fe^{2+}SOD is 8.50 ± 0.07 (*24*).

We were unable to accurately measure the p*K* of exogenous OH^- binding to Y34F-Fe^{3+}SOD because of spontaneous metal ion release from Y34F-Fe^{3+}SOD at pH > 8.7. The formation of orange inorganic precipitate (which presumably contained iron) was associated with this event, while >99% of the protein remained in solution. Proton NMR spectra of the apo-Y34F-FeSOD showed that the protein retained some structure as peaks upfield of 0 ppm were observed.

The partial pH titration of Y34F-Fe^{3+}SOD from pH 6.8 to 8.6 shows that A_{380} drops off more gradually than in the WT, as the maximum stable pH of ~8.7 is approached (Figure 7). This implies that hydroxide either binds with a higher p*K* to Y34F- than WT-Fe^{3+}SOD, or that the ϵ_{380} of

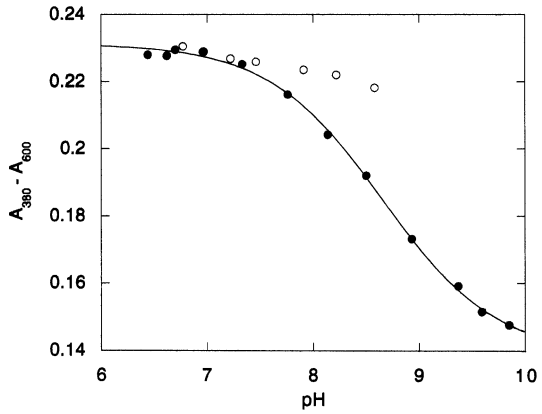

FIGURE 7: pH dependence of the absorbance of WT-Fe^{3+}SOD (●) and Y34F-Fe^{3+}SOD (○) at 380 nm, A_{380}. The absorbance at 380 nm was corrected for any baseline drift or protein precipitation by subtracting the absorbance at 600 nm, which is zero in native protein and pH independent. Protein was suspended in 10 mM CAPS, 10 mM PIPES, 10 mM NaCl. The fit to the Henderson−Hasselbalch equation is shown for WT-Fe^{3+}SOD, and the p*K* values obtained are listed in Table 3 and the text.

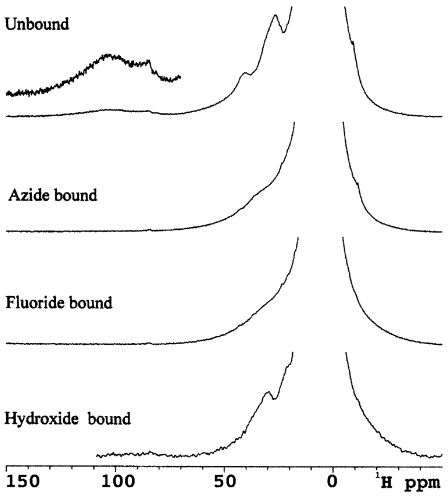

FIGURE 8: Anion binding to oxidized Fe^{3+}SOD. ^{1}H NMR super-WEFT spectra are compared for Fe^{3+}SOD at pH 6.0 (top), at pH 6.0 with 5 mM NaN_3 (second, the K_d for N_3^- is 1.5 mM), at pH 6.0 with 10 mM KF (third, the K_d for F^- is 2.0 mM), and at pH 9.3 (bottom, [OH^- bound]/[OH^- not bound] ≈5 based on p*K* of 8.6).

hydroxide-bound Y34F-Fe^{3+}SOD is greater than that of WT-. In an attempt to distinguish the two possibilities, the K_d of N_3^- binding to Y34F-Fe^{3+}SOD was redetermined at pH 8.7. If N_3^- and OH^- compete for a metal coordination site in Y34F-Fe^{3+}SOD as they do in the WT, the apparent K_d of azide binding should increase as pH increases, reaching $K_d^{apparent} = 2\ K_d$ when pH = p*K*. At pH 8.7 the apparent K_d of azide binding was found in two independent titrations to be 136 ± 24 μM and 170 ± 25 μM with an average value of 152 ± 17 μM, compared with 81 ± 15 μM at pH 7.4. This implies a p*K* of ~8.8 for OH^- binding, which is not significantly different from the wild-type value of 8.61, and therefore an ϵ_{380} of OH^--bound Y34F-Fe^{3+}SOD, which is greater than that of the WT.

The native-or-weaker binding of (smaller) F^- and OH^- to Y34F-Fe^{3+}SOD suggests that tighter binding of (larger) N_3^- does in fact represent relief of strain. Thus, Tyr34 appears to impose specificity in favor of substrate (analogues) smaller than three second-row atoms.

NMR Studies of Anion Binding to Fe^{3+}SOD. The active site ^{1}H NMR spectrum of (oxidized) Fe^{3+}SOD is much less resolved than that of (reduced) Fe^{2+}SOD, due to the slower electronic spin relaxation of Fe^{3+}, which causes faster proton relaxation (*3*, *36*). In the presence of N_3^- or F^- the ^{1}H NMR resonances of Fe^{3+}SOD in the 20−50 ppm range (ligand His α and/or β protons) are broadened nearly to the limit of detection, and resonances near 100 ppm (ligand His Nδ1 protons, (*33*)) are broadened beyond visibility (Figure 8). Additional resonances are observed to broaden in the 10 to 0 ppm range upon F^- and N_3^- binding (Vathyam and Miller, unpublished results). In the case of OH^- binding, broadening also occurs but to a lesser degree.

These paramagnetically shifted resonances' line widths are dominated by the paramagnetic contribution to the transverse proton relaxation rate $(1/T_2)_p$, which in Fe^{3+}SOD is expected to be proportional to the electron spin relaxation time.[4] Since electron spin relaxation times are longer in high spin Fe^{3+} sites with higher symmetry, the broadened lines confirm earlier conclusions that six-coordinate complexes are formed with F^-, N_3^-, or a second OH^- bound to Fe^{3+}. In this case, slowed electron spin relaxation should result in acceleration of the $1/T_1$ as well as the $1/T_2$ relaxation rates of all protons near the metal ion, including those of water or bound OH^-. Thus, our data show that enhanced ^{1}H relaxation can explain the increase in paramagnetic relaxation of water previously observed upon binding of N_3^- (*15*). However, because no increase in water relaxation was observed in the case of F^- binding, a second, canceling effect must be invoked.

Dooley et al. (*15*) proposed that bound N_3^-, but not F^-, might favor water binding near Fe, and thus mediate paramagnetic relaxation of water. However, we and Slykhouse and Fee (*11*) find that F^- can bind in two sites, whereas N_3^- appears to just bind once. Therefore, we propose that F^- binding in the second site replaces the normally bound water (Figure 1) or diminishes its exchange rate and thus explains the suppression of paramagnetic relaxation of water upon F^- binding. EPR data of Slykhouse and Fee support two forms of F^--bound Fe^{3+}SOD at low temperature (*11*). However, if the microscopic K_d's of the two F^- binding events are similar and the events responsible for the two K_d's are in fast equilibrium at room temperature, then spectroscopic changes due to each may not be separately observable. Two macroscopic K_d's would nonetheless be observed if the two binding events are anticooperative, and at F^- concentrations between the two macroscopic K_d's, approximately 50%

[4] In Fe^{3+}SOD, where the Fe^{3+} ion is tightly bound to the protein (exceedingly low dissociation rate, $1/\tau_M$), and the protein tumbles slowly due to its large size (low rotation rate, $1/\tau_r$), the electron spin correlation time τ_c is approximately equal to the electron spin relaxation time, which for octahedral high spin Fe^{3+} is $\tau_e \approx 10^{-10}$ s (*2*). Moreover, with this long τ_c, a proton Larmor frequency of $\omega_I = 1.9 \times 10^9\ s^{-1}$ and an electron frequency of $\omega_e \approx 1 \times 10^{12}\ s^{-1}$ for ^{1}H NMR at 300 MHz, most of the dispersive terms in $(1/T_2)_p$ are negligible and $(1/T_2)_p$ is proportional to τ_c, so the line widths of predominantly paramagnetically broadened lines are proportional to the electron spin relaxation time. For high spin Fe^{3+}, electron spin relaxation via low-lying excited states is more efficient in lower symmetry coordination geometries that stabilize one or more d orbitals, and thus make an excited state more energetically accessible (*2*). Therefore, expansion of Fe^{3+}SOD's coordination number from 5 (with trigonal bipyramidal geometry) to 6 (more closely approaching octahedral) is expected to increase τ_e, and thus τ_c and the paramagnetic NMR line widths $(1/T_2)_p$ (*2*−*4*).

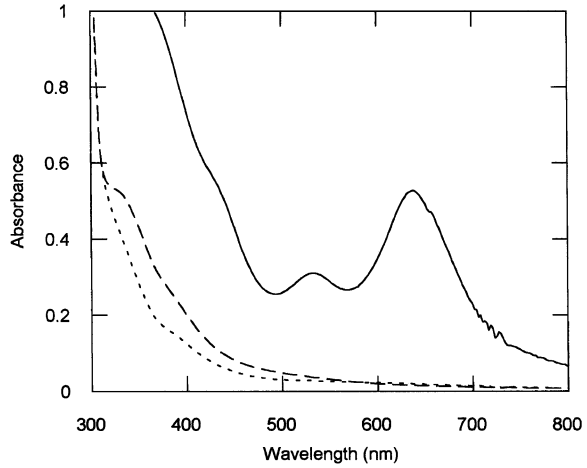

FIGURE 9: UV/vis spectra of FeSOD before (long dashes), immediately after (short dashes), and 20 h after (solid line) the addition of pH 7.4 SH^- to a final concentration of 50 mM.

of the whole spectroscopic change would be observed, as each site would be ~50% occupied. Furthermore, the nature and magnitude of a spectroscopic change associated with the second macroscopic K_d would be similar to those of the first. This is consistent with the two F^- binding events observed by UV/Vis spectroscopy for both WT- and Y34F-Fe^{3+}SOD. Thus, F^- may be able to coordinate to Fe^{3+} twice, like OH^-, and impede water access to Fe^{3+}.

Interaction of FeSOD with Hydrogen Sulfide. HS^- is another possible substrate analogue, as well as a plausible substitute for coordinated solvent. However, it is softer and more electron rich and therefore potentially amenable to oxidation. Indeed, we have found that HS^- interacts in a complex way with FeSOD. Upon addition of excess SH^-, the broad visible absorbance of Fe^{3+}SOD near 350 nm immediately disappeared and the enzyme became colorless (Figure 9). The colorless FeSOD displayed the same ^1H super-weft NMR spectrum as the native Fe^{2+}SOD active site, indicating that the color loss was due to reduction of the enzyme. Upon exposing SH^--reduced Fe^{2+}SOD to air, an intense green color gradually developed over a period of hours (Figure 9). Because the green species first appeared at the meniscus, oxygen is almost certainly responsible for its formation. Moreover, as the green color intensified, the intensity of the active site Fe^{2+}SOD ^1H NMR spectrum diminished, indicating that the formation of the green species involves reoxidation of FeSOD. The chromophore was confirmed to be tightly bound to the protein as the filtrate from membrane ultrafiltration was colorless, while the concentrated protein remained green.

The green species' UV/vis absorbance maxima at 636 and 530 nm reached maximal intensities after 1−2 days of exposure to air at 4 °C. At this point, extinction coefficients of $\epsilon_{636} = 3950\ cm^{-1}\ M^{-1}$ and $\epsilon_{530} = 2346\ cm^{-1}\ M^{-1}$ were calculated based on the total FeSOD concentration used. These values are only lower limits, as they assume that all the FeSOD was converted to the green species. The extinction coefficients and wavelengths are compatible with coordination of a sulfide (HS^-) or sulfinic acid ligand ($\sim SO_2^-$) (*37*).

The EPR signal of the green Fe^{3+}SOD complex clearly corresponds to a high spin Fe^{3+}, not low spin ($S = 1/2$), as the signal is concentrated in the region of $g' = 4.3$, not $g' = 2$ (Figure 10). With its single sharp derivative at $g' = 4.236$, the EPR signal of green Fe^{3+}SOD displays the least dispersed g' values near 4.3, of the Fe^{3+}SOD anion complexes. This suggests a close to ideal octahedral coordination environment for green Fe^{3+}SOD, and thus hexacoordination. The sample treated with F^- displays the signal characteristic of one F^- per active site (*11*), consistent with the concentration of F^- used and our measured K_d. We also note splitting potentially representing superhyperfine coupling to ^{19}F, of 26 G at $g' = 4.4$. Thus, we conclude that a novel high spin, six-coordinate Fe^{3+} species is formed in the active site of Fe^{3+}SOD, most likely representing coordination to Fe^{3+} of HS^- (or an oxidized derivative).

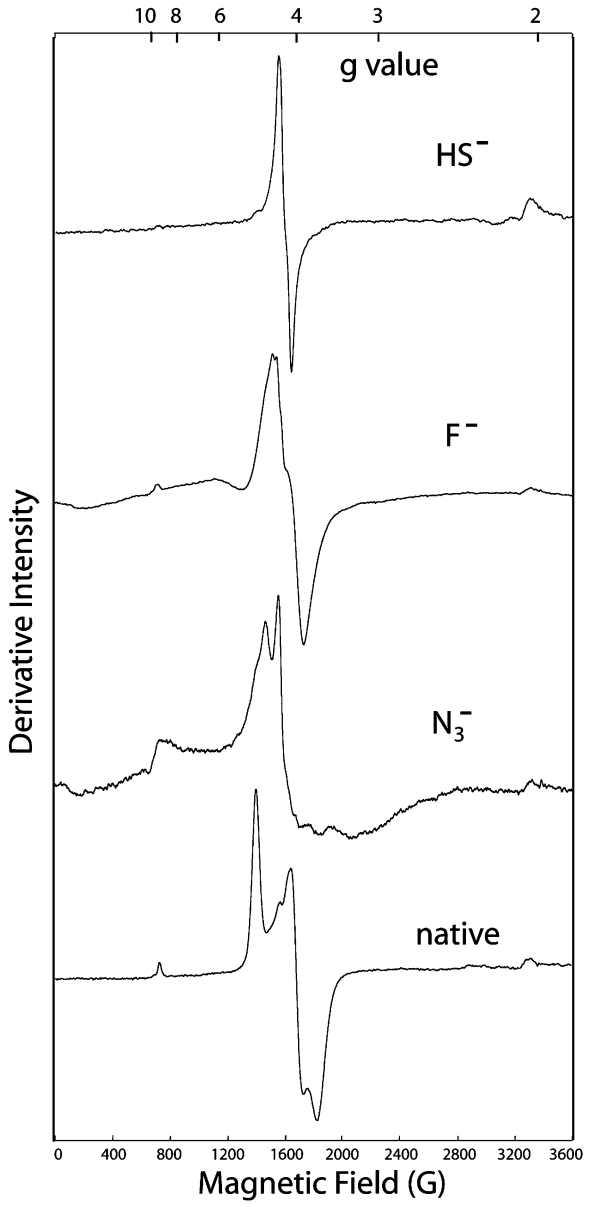

FIGURE 10: EPR spectra of native and anion-bound Fe^{3+}SOD. Samples of approximately 0.5 mM oxidized Fe^{3+}SOD suspended in 25 mM phosphate at pH 7.5 (or dialyzed into deionized water, for the HS^- study) were augmented with HS^- to 33 mM, F^- to 33 mM, N_3^- to 30 mM, or NaCl to 29 mM (in 5 mM phosphate), and frozen in liquid N_2. EPR conditions were as described in the methods.

As the green color developed, the ^1H NMR spectrum also changed, becoming most similar to the high pH spectrum of Fe^{2+}SOD. Indeed, we found that a pH increase from 7.4 to

as high as 10.5 accompanied the formation of the green species. Thus, Fe oxidation in the presence of HS^- is accompanied by H^+ uptake. Since this is contrary to the case for FeSOD alone, we propose that this reflects reactions involving the HS^-. Moreover, reoxidation was also accompanied by appearance of a whispy light-colored precipitate near the meniscus that was not protein but was consistent with elemental sulfur or insoluble polysulfides (S_n^{2-}), suggesting reactions such as $HS^- + O_2 + H^+ \rightarrow S^\circ + H_2O_2$ (*38*). Nonetheless, the fact that the dominant ^1H NMR signals observed could all be explained by known species suggests that neither HS^- nor its derivatives bind to Fe^{2+}SOD.

The chemistry of HS^- with O_2 is complicated and beyond the scope of this work. However, it is clear that HS^- interacts with FeSOD as a reagent, and HS^- or an oxidized product thereof can coordinate Fe^{3+}.

DISCUSSION

Substrate Analogue Bound-Reduced Fe^{2+}SOD. Prior to this work there was no spectroscopic observation of specific anion-binding to the active site of reduced Fe^{2+}SOD. Although substrate must somehow interact with Fe^{2+}SOD, MCD spectroscopy demonstrated that neither F^- nor N_3^- coordinates to the Fe^{2+} (*30*), and while NO has been shown to interact with Fe^{2+}SOD (*1*, *23*), the species that results is best interpreted as Fe^{3+}SOD coordinated by NO^- (*1*). Thus, the Fe^{3+}SOD·NO^- is really a model for the oxidized state of the enzyme not the reduced state. The fact that Fe^{3+}SOD·NO^- is formed nonetheless implies that NO does interact with the Fe in Fe^{2+}SOD, but it suggests that NO's coordination is associated with electron transfer, given the failure of redox-inert anions to coordinate to Fe^{2+}. Thus, the F^- bound state we have observed here is the first model for substrate interaction with reduced Fe^{2+}SOD.

An "Anion Binding Pocket". The existence of an "anion binding pocket" in FeSOD was first proposed by Fee et al. (*22*) and further developed by Benovic, Bull, and Fee (*6*, *19*) based upon the observations that various anions inhibit SOD activity and N_3^- binding without coordinating to Fe^{3+} themselves, and that N_3^- binding occurs in at least two distinct steps (*22*). Proposals call for this outer-sphere site to be empty in order for superoxide to bind productively, either because it is the site of a prebinding event or the space is needed for conformational changes associated with substrate binding, redox chemistry or protonation. However, Argese et al. concluded that *all* anions diminish access to the active site due simply to ionic strength effects (*18*). Here, we show that even noncoordinating anions do not all behave alike. Although 50 mM F^- produces significant changes in the ^1H spectrum of the active site of Fe^{2+}SOD, neither 50 mM N_3^- nor $^-$SCN does, at the same ionic strength. Moreover, the F^- titration agrees with a well-defined stoichiometry of one F^- per active site. Thus, some specificity applies to the interaction between F^- and Fe^{2+}SOD, and we favor the existence of an anion-binding pocket (*20*), albeit a weak one.

The large K_d of 42 mM demonstrates that relatively little energy is associated with the interaction between F^- and Fe^{2+}SOD's active site, which in turn precludes highly selective, highly localized binding in the conventional "all-or-none" sense.[5] Thus, it may be better to think of F^- as interacting preferentially with a region of the Fe^{2+}SOD active site, and having a higher-than-bulk concentration there. Nonetheless, similar behavior on the part of substrate could still suffice to bring it close enough to Fe^{2+} for long enough to considerably accelerate the rate of $O_2^{\bullet-}$ reduction by Fe^{2+}. Since the NMR spectral effects of F^- are similar to those associated with deprotonation of Tyr34, we conclude that F^- binding is also a second-sphere event.[6] Thus, our work provides the first positive evidence that substrate binding for reaction 2 may occur in the outer sphere, possibly in the anion-binding pocket.

Relation of Anion Binding to Tyr34 in Reduced Fe^{2+}SOD. Substrate has been proposed to approach the active site via a funnel that stops just short of the active site, with His30 and Tyr34 separating the Fe center from solvent access (*7*). Thus, Brownian dynamics have been suggested to be necessary to allow the substrate to contact Fe (*39*) and the "anion-binding pocket" may be located at the base of the funnel, just outside the Tyr34 gate, for example in the position of the noncoordinating crystallographic water observed for Fe^{2+}SOD (Figure 1). Sines et al. calculated that Tyr34's steric hindrance of substrate access to Fe could be slowing overall catalytic activity by a factor of 5 to 15 (*39*). However, the three Tyr34 mutants of FeSOD examined to date (Y34F, Y34S, and Y34C) each show slightly *decreased* activity (*28*). Thus, Tyr34 makes some additional positive contribution to catalytic activity which is not fulfilled by the replacements and which outweighs the effects of any steric hindrance.

Tyr34 is conserved in most Fe and MnSODs (*10*). Although it has been proposed to be a proton donor to substrate in reaction 2 (*6*, *16*), to mediate proton transfer to coordinated solvent from bulk, to mediate proton transfer from coordinated solvent to nascent H_2O_2, and to modulate the mode/geometry of substrate binding (*6*, *9*, *16*, *17*, *23*, *27*, *35*), either these functions are supported by other active site residues too, or they are not essential for turnover, as mutation of Tyr34 to Phe only decreases k_{cat}/K_M activity by half for *E. coli* FeSOD. Nonetheless, mutation of the analogous Tyr of *Sulfolobus solfataricus* to Phe produces a 17-fold decrease in activity under k_{cat}/K_M conditions (*25*), indicating that Tyr34 makes a significant nonduplicated contribution to activity in some FeSODs, at least. Therefore, we have investigated Tyr34's possible contributions to substrate binding, substrate specificity, and H-bond donation to substrate. Some mechanism for protonation of substrate is likely to be crucial for reaction 2.

In order for $O_2^{\bullet-}$ to be a good reductant of Fe^{3+} in reaction 1, it should not be strongly stabilized by a H-bond. However in order for reaction 2 to be possible, reduction of $O_2^{\bullet-}$ must be closely coupled to protonation of $O_2^{\bullet-}$ (*26*). Moreover, the identities of the O atoms that receive H-bonds are important to the outcome of $O_2^{\bullet-}$ reduction. Double protonation at the distal O would be expected to promote cleavage of the O−O bond, whereas protonation at the coordinated (proximal) O would favor dissociation of

[5] F^- may also interact with other regions of the protein, but by looking at only paramagnetically shifted and relaxed NMR resonances, we focus specifically on events that affect the active site.

[6] The insignificance of any NMR line width changes also rules out a large change in active site structure.

Scheme 2: Cartoon of Binding of Too-Large N_3^-, Sterically Impeded by Tyr34 vs Binding of Too-Small F^-, Aided by Tyr34, Compared to Possible Binding of $O_2^{\bullet-}$

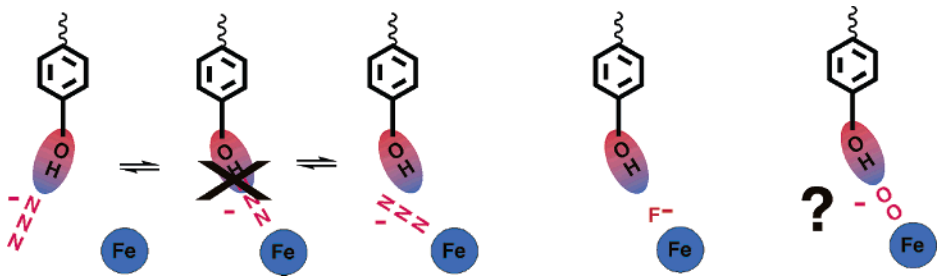

peroxide (*40*). Disruption of proton donation to that position could be a reason why mutation of residues affecting the H-bonding network of human MnSOD resulted in greater accumulation of a peroxide-bound inhibited intermediate (*8*, *41*). Thus, precise positioning as well as timing of proton transfer is crucial to SOD activity, and occasional misplacement of H-bonds may explain the accumulation of product-inhibited WT-MnSOD.

In the oxidized state the coordinated solvent is OH^-, whereas in the reduced state it is H_2O (*6*, *7*, *16*). Hence, the polarization of the active site H-bond network would be expected to change upon reduction, with less H-bond donation capability directed toward coordinated solvent and more available at the Tyr34 end for H-bond donation to incoming substrate, as required by the chemistry (*27*). Indeed, the p*K* of Tyr34 is only 8.5 in reduced Fe^{2+}SOD, whereas it is considerably higher in oxidized Fe^{3+}SOD (*42*). Thus, Gln69 and Tyr34 could together function to mediate effective proton transfer from coordinated solvent to nascent product (*43*), in concert with electron transfer from Fe^{2+}. However, our tests of this attractive proposal do not support strong H-bond donation from Tyr34 to substrate, as it binds to reduced Fe^{2+}SOD for reaction 2. Although our data show that Tyr34's phenolic proton is weakly beneficial based on the somewhat lower K_d for F^- binding to WT- vs Y34F-Fe^{2+}SOD, H-bond donation from Tyr34 is not required for F^- binding, even to reduced Fe^{2+}SOD.

Suppression of F^- binding at high pH appears instead to be due to the anion of (deprotonated) Tyr34 having an inhibitory effect. This could be simply electrostatic repulsion of the exogenous anion by the phenolate, consistent with our earlier finding that OH^- loses access to the active site of Fe^{2+}SOD upon Tyr34 ionization (*24*). Repulsion of anions would also decrease substrate access to the active site, thereby explaining the pH dependence of the K_M for reaction 2 (*44*). Electrostatic repulsion could similarly bar peroxide access to the active site, thus protecting FeSOD from inactivation (*8*, *9*) under conditions where it would not be catalytically active anyways, due to competitive inhibition of reaction 1 by OH^- binding (*24*) (but see ref *25*). Thus, Tyr34 can contribute to specificity against peroxide and in favor of substrate, by virtue of its intermediate p*K*.

The Nature of F^- Binding to Reduced Fe^{2+}SOD. The competition between F^- binding vs ionization of Tyr34, and the effect of F^- on backbone chemical shifts of residues 35−40 (*20*), most simply suggest that F^- occupies a site close to Tyr34. In addition, the active site NMR spectrum changes in similar ways upon deprotonation of Tyr34 and F^- binding (in either WT- or Y34F-Fe^{2+}SOD), suggesting that both events have similar effects (Figures 2 and 4). Specifically, the absence of line width changes argues against an inner-sphere event or gross structural change. However, the inclusiveness of the spectral changes suggests that they reflect changes in the paramagnetic contributions to chemical shift, which would change (to varying extents) for all paramagnetically affected resonances, rather than the diamagnetic contribution, which would be affected only for one or two residues that directly interact with F^-. In addition, the effects are moderately large compared to changes expected for the diamagnetic chemical shift (up to 3 ppm, vs less than 1 ppm, respectively). Thus, it appears that deprotonation of Tyr34 and binding of F^- cause similar effects on the polarization of Fe^{2+} d-electron density. This too could simply reflect electrostatics, if F^- is concentrated in the same region as that occupied by $Tyr34^-$'s phenolic O^- upon Tyr34 ionization.

Anion Binding Involving Coordination to (Oxidized) Fe^{3+}. We find that N_3^- binds 19-fold more *tightly* to oxidized Y34F-Fe^{3+}SOD than to the WT- and appears to have a stronger coordination to Fe^{3+} (Figure 6 and refs *9* and *17*), in good agreement with the finding that N_3^- inhibits the activity of Y34F-FeSOD with a 20-fold lower K_I than the WT- (*28*) and the accepted view that N_3^- inhibits by coordinating to Fe^{3+} (*6*). The smaller anions OH^- and F^-, by contrast, bind to Y34F-Fe^{3+}SOD up to 5 times (F^-) more *weakly* than they bind to WT. Thus, our data suggest that N_3^-'s larger size constrains it to an orientation/position that compromises its interaction with Fe^{3+} in WT-Fe^{3+}SOD. For OH^-, the optical signature of binding is weaker in Y34F-Fe^{3+}SOD, in addition to the marginally larger K_d. Thus, for both large and small anions, the more favorable interaction with residue 34 is associated with better coordination to Fe^{3+}. Moreover at high pH, Fe^{3+} escapes from the active site in Y34F- but not WT-Fe^{3+}SOD. Thus, Tyr34 appears to provide an anchor or barrier that holds onto $Fe^{3+}(OH^-)_2$, along with the three His and Asp^- ligands.

In summary, we envision a binding site with contributions from both Tyr34 and Fe^{3+}, positioned with a separation that is too small to accommodate N_3^- comfortably, yet able to aid each other (weakly) in OH^- and F^- binding. Such an arrangement might be "just right" for a diatomic molecule and thus support the significantly lower K_M of 100 μM for $O_2^{\bullet-}$ (*6*) than the K_d's of 1.5 mM for F^- and 2 mM for N_3^-.[7]

Different Contributions to Substrate Analogue Binding. To evaluate Tyr34's possible significance to substrate

[7] The K_M for $O_2^{\bullet-}$ is in fact an overestimate for the K_d as the former will be increased by the forward reaction rate. The similarity between the WT K_M for $O_2^{\bullet-}$ and the K_d for N_3^- binding to Y34F-FeSOD nonetheless suggests that sterics represent the main difference between binding to WT and Y34F-Fe^{3+}SOD.

binding, one would like to be able to separate and evaluate different elements of this event. Our current measurements allow us to address (1) coordination to Fe (observed for Fe^{3+}, not Fe^{2+}), (2) steric clash with Tyr34's OH, and (3) H-bonding to Tyr34's OH. Since mutation of Tyr34 to Phe eliminates the latter two at once, we have also addressed steric constraints by comparing binding of anions of different size. Although the reduced state appears to employ a different substrate binding mode, any differences in the applicable steric constraints are expected to be minimal for the small anion F^-, since it appears relatively exempt from steric repulsion.[8] Indeed, since F^- binding is weaker in Y34F-Fe^{2+}-SOD than in WT-, steric effects appear smaller than the lost benefits of any H-bond. However, we nonetheless recognize that steric effects may not be zero by referring to "net H-bonding", meaning actual H-bonding effects minus effects of steric repulsion. Thus, we begin with a simple model in which the free energy of anion binding to FeSOD, ΔG_b, is made up of a favorable (negative) contribution from coordination to Fe^{3+}, ΔG_{Fe}, an unfavorable (positive) contribution from steric conflict with Tyr34, ΔG_{ster}, and a favorable (negative) contribution from H-bond donation from Tyr34, ΔG_{Hbd}.

$$\Delta G_b = \Delta G_{Fe} + \Delta G_{ster} + \Delta G_{Hbd}$$
$$\Delta G_b = -2.3RT\log(K_b) = 2.3RT\log(K_d) \quad (9)$$

where additional subscripts will be used to indicate the oxidation state, anion identity, and protein identity under consideration, and K_b and K_d denote the binding constant and the dissociation constant for anion binding, respectively.

In Fe^{2+}SOD, where anions do not coordinate to Fe, we set $\Delta G_{Fe} \approx 0$, and for the small anion F^- we set $\Delta G_{ster} \approx 0$. Thus, for this simplest case, the net contribution of H-bonding with Tyr34 may be roughly estimated from the loss of binding affinity produced by mutating Tyr34:

$$\Delta G_{Hbd,2+,F} \approx \Delta G_{b,2+,F,WT} - \Delta G_{b,2+,F,Y34F} = 2.3RT\log(42/66) = -1.1 \text{ kJ/mol.}^8$$

In comparison, the net contribution of H-bonding with Tyr34 appears larger for the oxidized state:

$$\Delta G_{Hbd,3+,F} \approx \Delta G_{b,3+,F,WT} - \Delta G_{b,3+,F,Y34F} = 2.3RT\log(2/10) = -3.9 \text{ kJ/mol}$$

Thus, H-bonding to Tyr34 and coordination to Fe^{3+} are mutually cooperative in the amount of 2.8 kJ/mol, and binding to either Tyr34 or Fe^{3+} effectively raises the local F^- concentration 3-fold.

$\Delta G_{Fe,F}$, the free energy associated with F^- coordination to Fe^{3+}, can be estimated by assuming that binding of F^- to the Fe^{3+} and Fe^{2+} forms of Y34F-FeSOD involves similar values for $\Delta G_{ster} + \Delta G_{Hbd}$ (both ≈ 0). Thus,

$$\Delta G_{Fe,F} \approx \Delta G_{b,3+,F,Y34F} - \Delta G_{b,2+,F,Y34F} = 2.3RT\log(10/66) = -4.6 \text{ kJ/mol}$$

Hence, it appears that when steric conflict is small, Fe^{3+} is responsible for most of the binding affinity. By comparison, the net contribution of H-bonding from Tyr34 in the absence of coordination to Fe^{3+} is very modest (-1.1 kJ.mol), but its cooperative reinforcement of coordination to Fe^{3+} is significant ($> kT \approx 2.5$ kJ/mol).[9] Since neither OH^- nor N_3^- binds to WT-Fe^{2+}SOD, no additional values can be obtained. Moreover, this is probably an unavoidable manifestation of the small value of $\Delta G_{Hbd,2+}$, since for larger anions, sterics (or ionization of Tyr34 at high pH) will outweigh such a weak binding interaction.

The contribution of sterics to binding to Fe^{3+}SOD was not estimated from a comparison of N_3^- binding and F^- binding because this would assume similar Fe^{3+} coordination strengths for two quite different anions. Instead, we thought the strength of H-bonding would be less different for the two anions,[10] and subtracted this (determined in the reduced state for F^-) from the total effect of mutating Tyr34 to Phe observed for N_3^- binding (sterics + H-bonding), to estimate the contribution of sterics.

$$\Delta G_{ster,3+} \approx (\Delta G_{b,3+,N3,WT} - \Delta G_{b,3+,N3,Y34F}) - \Delta G_{Hbd,3+,F} = 2.3RT\log(1.5/0.08) + 1.1 \text{ kJ/mol} \approx 7.1 \text{ kJ/mol} + 1.1 \text{ kJ/mol} = 8.2 \text{ kJ/mol}$$

This value is a very rough estimate only because the steric interference between Tyr34 and N_3^- most likely precludes the formation of any H-bond (*7*), so that the more conservative $\Delta G_{ster} \approx 7$ kJ/mol is probably a better value.

In summary, our very limited data provide estimates for three different contributions to substrate analogue binding, collected in Table 4. While these should be viewed strictly as a starting point to be tested if possible with data from additional anions and mutants, they nonetheless suggest that H-bond donation from Tyr34 in the reduced state is less significant than steric repulsion of oversize substrate analogues and electrostatic repulsion of anions at pHs above 8.5. The absence of a pH effect on k_{cat} further argues against Tyr34's making an important H-bonding contribution to the transition state, although its bulk may help to constrain the position and orientation of bound substrate in MnSOD (*45*) and may favor product dissociation. Our current data also suggest that Tyr34 may play an important role in excluding non-substrate anions, in particular peroxide, and thus may suppress spurious Fenton chemistry under conditions of oxidative stress (*8*, *9*, *24*, but see ref *25*).

Interaction of FeSOD with Hydrogen Sulfide. HS^- has been shown to interact with Cu,ZnSOD by Searcy and colleagues and moreover to support multiple turnovers of the enzyme as an alternative reductant to $O_2^{\bullet -}$ (*38*, *46*). As

[8] Since we have assumed that for the reduced state, $\Delta G_{Fe} \approx 0$ and we are assuming that for small anions $\Delta G_{ster} \approx 0$, even this small ΔG_{Hbd} energy becomes significant. It does not reflect the full binding energy since F^- binds even to Y34F-Fe^{2+}SOD, which lacks the capacity to donate this H-bond. Other contributions may derive from H-bonding from His30, for example.

[9] Similarly, when H-bonding from Tyr34 is present, $\Delta G_{Fe,F,WT} \approx 2.3RT\log(K_{d,3+,F,WT}/K_{d,2+,F,WT}) = 2.3RT\log(2/42) = -7.4$ kJ/mol. As expected, this value is 2.8 kJ/mol more favorable than the contribution to binding of Fe^{3+} alone, of -4.6 kJ/mol.

[10] Although the p*K*'s of HF and HN_3 are slightly different (HN_3's p*K* is 4.6 and HF's is 3.2), we assume as a starting point that their H-bonds with Tyr34 may have comparable strengths.

Table 4: Estimates of Different Contributions to Anion Binding in WT-FeSOD, in kJ/mol

interaction	sterics for N_3^- (for Fe^{3+})	H bonding with Tyr34 (for F^-)	F^- coordination to Fe^{3+}	cooperativity (Hbd vs Fe^{3+}), F
free energy	+7.1	−1.1	−4.6	−2.8

for FeSOD, a complex in which HS^- is coordinated to the active site Cu^{2+} ion was identified (*46*).

For FeSOD, further experiments addressing stoichiometries and nature of the reaction with O_2 will be necessary to resolve the potentially very complex chemistry occurring with HS^-. However, the most likely explanation for the green species is coordination of HS^- or an oxidation product thereof to Fe^{3+}. Indeed, whereas our green Fe^{3+}SOD complex has absorption maxima at 530 and 636 nm ($\epsilon \geq 2300$ and 4000 M^{-1} cm^{-1}, respectively), Fe^{3+} complexes with similar absorption maxima have been reported. For example: maxima at 540 and 650 nm for a trigonal bipyramidal Fe^{3+} coordinated by two thiolates, one pyridine N, and two deprotonated amide Ns ($\epsilon \approx 3600$, 3700 M^{-1} cm^{-1}, *47*), and others tabulated by Kovacs (*37*). However, the above complex is five-coordinate, whereas our green FeSOD appears to be six-coordinate based on EPR at 110 K (Figure 10) 16 and 4.2 K (not shown). Furthermore, upon coordinating a sixth ligand the above complex becomes low spin, like other multi-thiolate or multi-sulfinate complexes, and nitrile hydratase (*37*), whereas green Fe^{3+}SOD is high-spin, again based on our EPR spectra, obtained at 110, 16, and 4 K.

Our green Fe^{3+}SOD displays strong parallels with the active site of oxidized superoxide reductase (SOR), which binds Fe^{3+} with one Glu^- and four histidines, similar to FeSOD's Asp^-·His_3 site. However, the SOR site also contributes one Cys thiolate ligand to Fe^{3+}. Fe^{3+}SOR has an absorption maximum at 660 nm with $\epsilon \approx 2500$ M^{-1} cm^{-1} and an additional electronic band at 530 nm visible in the MCD spectrum at low temperature (*48*), very similar to the wavelengths represented in the optical spectrum of our green Fe^{3+}SOD. Moreover, based on optical, MCD, and EPR spectroscopy at a range of temperatures, these bands have been assigned to sulfur-to-Fe^{3+} charge transfer transitions with the intensity of the in-plane "sigma-type" transition (near 530 nm) depending strongly on the angle of the Cys C−S−Fe^{3+} bonds (*48*). Therefore, the weaker optical absorbance at 530 nm in SOR can be explained by different thiolate geometry from that in green Fe^{3+}SOD. Finally, SOR is high-spin and remains so upon binding N_3^- or F^-, like Fe^{3+}SOD. Thus, based on the data in hand, our Fe^{3+}SOD site bears stronger resemblance to the site with the more similar amino acid ligand set and only one thiolate ligand, and we tentatively assign our green Fe^{3+}SOD to a six-coordinate Fe^{3+} with one HS^- coordinated to Fe^{3+}.

CONCLUDING REMARKS

The results shown here demonstrate that HS^- can bind to Fe^{3+} and engage in redox reactions with it, making this a potentially informative model for the reactivity of FeSOD. F^- has been shown to bind to the reduced Fe^{2+}SOD active site without coordinating to Fe^{2+}, providing the first evidence for substrate analogue binding to Fe^{2+}SOD and supporting the existence of an "anion binding pocket" as well as an outer sphere mechanism for reaction 2. Tyr34 deprotonation competitively prevents F^- from binding. We propose that ionization of Tyr34 likewise prevents superoxide binding at high pH, explaining the pH dependence of the K_M of reaction 2. In addition, our comparisons of factors affecting FeSOD's affinity for large and small substrate analogues demonstrate that Tyr34 also imposes steric restrictions on substrate analogue access to the active site. Finally, by using protein ^1H NMR to infer changes in electron spin correlation time we have proposed a new explanation for the different effects on solvent relaxation of N_3^- and F^- binding to oxidized Fe^{3+}-SOD (*15*), in terms of binding of two F^- per Fe^{3+} vs one N_3^-, and hence potential displacement of the coordinated solvent by one F^-. Thus, we demonstrate the existence of several binding sites or binding modes, and multiple effects on binding affinity by Tyr34. Our data do not support H-bond donation from Tyr34 coupled to substrate binding but instead support a role for Tyr34 in enforcing substrate specificity.

ACKNOWLEDGMENT

We thank Prof. J. A. Fee for generously providing us with the gene for Y34F-FeSOD, and Mssrs. A. Sebesta and A. Floyd for tireless help maintaining equipment.

NOTE ADDED IN PROOF

Although even 50 mM N_3^- does not interact perceptibly with WT-Fe^{2+}SOD, we find that it binds to Y34F-Fe^{2+}SOD, with an (uncertainty^{-2})-weighted average K_d of 2.6 ± 0.5 mM. Thus, mutation of Tyr34 increases the binding site's capacity, enabling it to bind a triatomic substrate analogue, not just the monatomic F^- that binds to WT. The K_d is at least 40 times smaller than that of WT (>100 mM), indicating that Tyr34 imposes a similar net steric cost on N_3^- binding in both oxidation states. Thus, the reduced state is similar to the oxidized state in that mutation of Tyr34 to Phe weakens binding of small substrates (loss of an H-bond in the absence of steric penalty) but strengthens binding of larger substrates (subject to strong steric penalty).

REFERENCES

1. Jackson, T. A., Yikilmaz, E., Miller, A.-F., and Brunold, T. C. (2003) Spectroscopic and Computational Study of a Non-Heme Iron {Fe−NO}7 System: Exploring the Geometric and Electronic Structures of the Nitrosyl Adduct of Iron Superoxide Dismutase, *J. Am. Chem. Soc. 125*, 8348−8363.
2. Bertini, I., and Luchinat, C. (1986) *NMR of Paramagnetic Substances*, Vol. 150, Elsevier, Amsterdam.
3. LaMar, G. N., Horrocks, W. D., Jr., and Holm, R. H. (1973) *NMR of Paramagnetic Molecules*, Academic Press, New York.
4. Drago, R. S. (1992) *Physical Methods for Chemists*, Saunders College Publishing, New York.
5. Han, W. G., Lovell, T., and Noodleman, L. (2002) Coupled redox potentials in manganese and iron superoxide dismutases from reaction kinetics and density functional/electrostatics calculations, *Inorg. Chem. 41*, 205−218.
6. Bull, C., and Fee, J. A. (1985) Steady-State Kinetic Studies of Superoxide Dismutases: Properties of the Iron Containing Protein from *Escherichia coli*, *J. Am. Chem. Soc. 107*, 3295−3304.
7. Lah, M. S., Dixon, M. M., Pattridge, K. A., Stallings, W. C., Fee, J. A., and Ludwig, M. L. (1995) Structure−Function in *E. coli* Iron Superoxide Dismutase: Comparisons with the Manganese Enzyme from *T. thermophilus*, *Biochemistry 34*, 1646−1660.
8. Guan, Y., Hickey, M. J., Borgstahl, G. E. O., Hallewell, R. A., Lepock, J. R., O'Connor, D., Hsieh, Y., Nick, H. S., Silverman, D. N., and Tainer, J. A. (1998) Crystal Structure of Y34F Mutant

Human Mitochondrial Manganese Superoxide Dismutase and the Functional Role of Tyrosine 34, *Biochemistry 37*, 4722−4730.
9. Whittaker, M. M., and Whittaker, J. W. (1997) Mutagenesis of a proton linkage pathway in *Escherichia coli* manganese superoxide dismutase, *Biochemistry 36*, 8923−8931.
10. Wintjens, R., Noël, C., May, A. C. W., Gerbod, D., Dufernez, F., Capron, M., Viscogliosi, E., and Rooman, M. (2004) Specificity and phenetic relationships of iron- and manganese-containing superoxide dismutases on the basis of structure and sequence, *J. Biol. Chem. 279*, 9248−9254.
11. Slykhouse, T. O., and Fee, J. A. (1976) Physical and Chemical Studies on Bacterial Superoxide Dismutases, *J. Biol. Chem. 251*, 5472−5477.
12. Fee, J. A., McClune, G. J., Lees, A. C., Zidovetzki, R., and Pecht, I. (1981) The pH Dependence of the Spectral and Anion Binding Properties of Iron Containing Superoxide Dismutase from *E. coli* B: An Explanation for the Azide Inhibition of Dismutase Activity, *Isr. J. Chem. 21*, 54−58.
13. Tierney, D. L., Fee, J. A., Ludwig, M. L., and Penner-Hahn, J. E. (1995) X-ray Absoption Spectroscopy of the Iron Site in the *E. coli* Fe(III) Superoxide Dismutase., *Biochemistry 34*, 1661−1668.
14. Misra, H. P., and Fridovich, I. (1978) Inhibition of Superoxide Dismutases by Azide, *Arch. Biochem. Biophys. 189*, 317−322.
15. Dooley, D. M., Jones, T. F., Karas, J. L., McGuirl, M. A., Brown, R. D., III., and Koenig, S. H. (1987) Azide and Fluoride Binding to *E. coli* Iron Superoxide Dismutase as Studied by Solvent Proton Magnetic Relaxation Dispersion, *J. Am. Chem. Soc. 109*, 721−725.
16. Stallings, W. C., Metzger, A. L., Pattridge, K. A., Fee, J. A., and Ludwig, M. L. (1991) Structure−Function Relationships in Iron and Manganese Superoxide Dismutases, *Free Radical Res. Commun. 12−13*, 259−268.
17. Jackson, T. A., Xie, J., Yikilmaz, E., Miller, A.-F., and Brunold, T. C. (2002) Spectroscopic and Computational Studies on Iron and Manganese Superoxide Dismutases: Nature of the Chemical Events Associated with Active Site p*K*s, *J. Am. Chem. Soc. 124*, 10833−10845.
18. Argese, E., Orsega, E. F., Granito, C., and Moretto, L. M. (1995) A polarographic study of the catalytic mechanism of hte iron-containing superoxide dismutase from *Escherichia coli*, *Bioelectrochem. Bioenerg. 38*, 397−400.
19. Benovic, J., Tillman, T., Cudd, A., and Fridovich, I. (1983) Electrostatic Facilitation of the Reaction Catalyzed by the Manganese-Containing and the Iron-Containing Superoxide Dismutases, *Arch. Biochem. Biophys. 221*, 329−332.
20. Vathyam, S., Byrd, R. A., and Miller, A.-F. (2000) Mapping the effects of metal ion reduction and substrate analog binding to Fe-superoxide dismutase by NMR, *Magn. Reson. Chem. 38*, 536−542.
21. Sorkin, D. L., Duong, D. K., and Miller, A.-F. (1997) Mutation of Tyrosine 34 to Phenylalanine Eliminates the Active Site p*K* of Reduced Fe−SOD, *Biochemistry 36*, 8202−8208.
22. Fee, J. A., McClune, G. J., O'Neill, P., and Fielden, E. M. (1981) Saturation Behavior of Superoxide Dismutation Catalyzed by the Iron Containing Superoxide Dismutase of *E. coli*, *Biochem. Biophys. Res. Commun. 100*, 377−384.
23. Niederhoffer, E. C., Fee, J. A., Papaefthymiou, V., and Münck, E. (1987) in *Isotope and Nuclear Chemistry Division, Annual Report*, pp 79−84, Los Alamos National Laboratory, Los Alamos, NM.
24. Sorkin, D. L., and Miller, A.-F. (1997) Observation of a Long-Predicted Active Site p*K* in Fe-Superoxide Dismutase from *E. coli*, *Biochemistry 36*, 4916−4924.
25. Gogliettino, M. A., Tanfani, F., Scire, A., Ursby, T., Adinolfi, B. S., Cacciamani, T., and De Vendittis, E. (2004) The role of Tyr41 and His155 in the functional properties of superoxide dismutase from the archeon *Sulfolobus solfataricus*, *Biochemistry 43*, 2199−2208.
26. Sawyer, D. T., Gibian, M. J., Morrison, M. M., and Seo, E. T. (1978) On the Chemical Reactivity of Superoxide Ion, *J. Am. Chem. Soc. 100*, 627−628.
27. Miller, A.-F. (2001) in *Handbook of Metalloproteins* (Wieghardt, K., Huber, R., Poulos, T. L., and Messerschmidt, A., Eds.) pp 668−682, Wiley and Sons, Chichester.
28. Hunter, T., Ikebukuro, K., Bannister, W. H., Bannister, J. V., and Hunter, G. J. (1997) The Conserved Residue Tyrosine 34 Is Essential for Maximal Activity of Iron-Superoxide Dismutase from *Escherichia coli*, *Biochemistry 36*, 4925−4933.
29. Inubishi, T., and Becker, E. T. (1983) Efficient Detection of Paramagnetically Shifted NMR Resonances by Optimizing the WEFT Pulse Sequence, *J. Magn. Reson. 51*, 128−133.
30. Whittaker, J. W., and Solomon, E. I. (1988) Spectroscopic Studies on Ferrous Non-Heme Iron Active Sites: Magnetic Circular Dichroism of Mononuclear Fe Sites in Superoxide Dismutase and Lipoxygenase, *J. Am. Chem. Soc. 110*, 5329−5339.
31. Ming, L.-J., Lynch, J. B., Holz, R. C., and Que, L., Jr. (1994) One- and Two-Dimensional ^{1}H NMR Studies of the Active Site of Iron(II) Superoxide Dismutase from *Escherichia coli*, *Inorg. Chem. 33*, 83−87.
32. Renault, J. P., and Morgenstren-Badarau, I. (1999) Thermochromic Conformational Change of *Methanobacterium thermoautotrophicum* Iron Superoxide Dismutase, *Inorg. Chem. 38*, 614−615.
33. Sorkin, D. L., and Miller, A.-F. (2000) Amino-Acid-Specific Isotopic Labeling and Active Site NMR Studies of Iron(II)- and Iron(III)-Superoxide Dismutase from *Escherichia coli*, *J. Biomol. NMR 17*, 311−322.
34. Scarrow, R. C., Trimitsis, M. G., Buck, C. P., Grove, G. N., Cowling, R. A., and Nelson, M. J. (1994) *Biochemistry 33*, 15023−15035.
35. Miller, A.-F., Padmakumar, K., Sorkin, D. L., Karapetian, A., and Vance, C. K. (2003) Proton-Coupled Electron Transfer in Fe−Superoxide Dismutase and Mn−Superoxide Dismutase, *J. Inorg. Biochem. 93*, 71−83.
36. Bertini, I., Turano, P., and Vila, A. J. (1993) Nuclear Magnetic Resonance of Paramagnetic Metalloproteins, *Chem. Rev. 93*, 2833−2932.
37. Kovacs, J. A. (2004) Synthetic analogues of cysteinate-ligated non-heme iron and non-corrinoid cobalt enzymes, *Chem. Rev. 104*, 825−848.
38. Searcy, D. G. (1996) HS-:O_2 Oxidoreductase Activity of Cu,Zn Superoxide Dismutase, *Arch. Biochem. Biophys. 334*, 50−58.
39. Sines, J., Allison, S., Wierzbicki, A., and McCammon, J. A. (1990) Brownian Dynamics Simulation of the Superoxide-Superoxide Dismutase Reaction: Iron and Manganese Enzymes, *J. Phys. Chem. 94*, 959−961.
40. Loew, G. H., and Harris, D. L. (2000) Role of the heme active site and protein environment in structure, spectra, and function of the cytochrome P450s, *Chem. Rev. 100*, 407−419.
41. Hearn, A. S., Stroupe, M. E., Cabelli, D. E., Lepock, J. R., Tainer, J. A., Nick, H. S., Silverman, D. S. (2001) Kinetic Analysis Of Product Inhibition In Human Manganese Superoxide Dismutase, *Biochemistry 40*, 12051−12058.
42. Maliekal, J., Karapetian, A., Vance, C., Yikilmaz, E., Wu, Q., Jackson, T., Brunold, T. C., Spiro, T. G., and Miller, A.-F. (2002) Comparison and Contrasts between the Active Site p*K*s of Mn−Superoxide Dismutase and those of Fe−Superoxide Dismutase, *J. Am. Chem. Soc. 124*, 15064−15075.
43. Edwards, R. A., Whittaker, M. M., Whittaker, J. W., Baker, E. N., and Jameson, G. B. (2001) Outer sphere mutations perturb metal reactivity in manganese superoxide dismutase, *Biochemistry 40*, 15−27.
44. Terech, A., Pucheault, J., and Ferradini, C. (1983) Saturation Behaviour of the Manganese-Containing Superoxide Dismutase from *Paracoccus Denitrificans*, *Biochem. Biophys. Res. Commun. 113*, 114−120.
45. Jackson, T. A., Karapetian, A., Miller, A.-F., and Brunold, T. C. (2004) Spectroscopic and Computational Studies of the Azide-Adduct of Manganese Superoxide Dismutase: Definitive Assignment of the Ligand Responsible for the Low-Temperature Thermochromism, *J. Am. Chem. Soc. 126*, 12477−12491.
46. Searcy, D. G., Whitehead, J. P., and Maroney, M. J. (1995) Interaction of Cu, Zn Superoxide Dismutase with Hydrogen Sulfide, *Arch. Biochem. Biophys. 318*, 251−263.
47. Noveron, J. C., Olmstead, M. M., and Mascharak, P. K. (2001) A Syntheitc Analogue of the Active Site of Fe-Containing Nitrile Hydratase with Carboxamide N and Thioloato S as Donor: Synthesis, Structure and Reactivities, *J. Am. Chem. Soc. 123*, 3247.
48. Clay, M. D., Jenney, F. E., Jr., Hagedoorn, P. L., George, G. N., Adams, M. W. W., and Johnson, M. K. (2002) Spectroscopic studies of *Pyrococcus furiosus* superoxide reductase: implications for active-site structures and the catalytic mechanism, *J. Am. Chem. Soc. 124*, 788−805.

BI0476331